Relation of domain properties to structural changes in perpendicularly magnetized ultrathin films

M. J. Dunlavy and D. Venus
Department of Physics and Astronomy, McMaster University, Hamilton, Ontario, Canada
(Received 8 February 2000; revised manuscript received 10 May 2000)

The influence of interface mixing upon the magnetic domain properties in perpendicularly magnetized ultrathin films has been studied using Fe/2 ML Ni/W(110) samples. Annealing of films with an Fe thickness of 1–1.5 ML produces interface mixing that can be quantified using Auger electron spectroscopy, and related to the changes in domain properties (such as the activation energy for domain wall pinning, the domain correlation length, and domain concentration) as measured by the low frequency ac magnetic susceptibility. Analysis of the susceptibility, as well as model calculations of the magnetic anisotropy, suggest that pinning is caused by the perturbation of the domain wall energy by monolayer steps in thickness. Initially, annealing smooths the film, thus increasing the domain correlation length and activation energy. Further annealing causes mixing at the Fe/Ni interface, which reduces the anisotropy, thus reducing the activation energy and increasing the domain concentration. Annealing above 550 K breaks up the film and there is no magnetic response in the measurable temperature range.

I. INTRODUCTION

The formation and dynamics of magnetic domain walls are central to the practical magnetic properties of many ferromagnetic materials. Ultrathin magnetic films [$\leqslant 10$ atomic layers or monolayers (ML)] are no exception, and the existence and expression of fascinating magnetic phenomena such as low-dimensional critical behavior, perpendicular magnetic anisotropy, and the spin reorientation transition are intimately tied to the behavior of domains. In order to better understand these phenomena, it is necessary to understand the relationship of the domain properties to the structural properties specific to ultrathin films, such as thickness, roughness, and interface formation. A simple and versatile characterization of this relationship is through the concept of thermally activated pinning of domain walls by structural or magnetic inhomogeneities. While this general model has been applied with success to ultrathin magnetic films, there have been few systematic experimental studies of the link between model parameters, such as activation energy and pinning length, and relevant structural properties of the film, such as roughness, chemical mixing at interfaces, epitaxy, structural domains, and terraces.

Ultrathin films which are spontaneously magnetized perpendicular to the surface are well suited to the investigation of these issues. These films form domains spontaneously[1–4] because the magnetic dipole interaction between distant perpendicularly oriented spins is antiferromagnetic.[5] A large range of domain densities is accessible by variation of the film thickness or temperature.[2] Recent studies of perpendicularly-magnetized films have characterized the domains using hysteresis loops,[6–8] spatial images of the domains,[9–12] magnetic relaxation,[13,14] and the magnetic susceptibility.[15–17] A number of theoretical papers have investigated the link between the domain properties and the fine structure of the film, with particular emphasis on film roughness.[18–20] Others have linked domain formation in these systems to both the transition from ferromagnetism to paramagnetism[21] and the spin reorientation transition.[2,3]

This report concentrates on the effect of surface roughness and interface mixing on the formation and motion of domain walls in Fe films grown on a 2 ML Ni/W(110) substrate. Previous results[16] have shown that the low frequency ac magnetic susceptibility of these films is dominated by the response of the domain walls. The temperature-dependent measurements may be analyzed quantitatively to yield the activation energy for domain wall motion, the mean domain pinning length, and the temperature-dependent rate of domain formation. The variation of the domain properties with thickness was found to be controlled principally by the explicit dependence of the magnetic anisotropy upon thickness.[8] As has been shown for films magnetized in-plane,[22,23] susceptibility measurements are also very sensitive to structural changes. The present experiments investigate the effect of interface integrity and mixing on perpendicularly magnetized films of constant thickness, by using step-wise annealing. The analysis shows that it is the effect of interface mixing on the magnetic anisotropy which is the dominant influence on domain properties. This makes it clear that it is not only surface roughness which is important in the domain dynamics of ultrathin films and multilayers, but chemical mixing at interfaces as well.

II. THE CONTRIBUTION OF DOMAIN WALL MOTION TO THE MAGNETIC SUSCEPTIBILITY

The magnetic susceptibility $\chi(T)$ of a perpendicularly magnetized ferromagnetic film results almost entirely from the motion of domain walls. This is the result of two effects that can be traced to the magnetic dipole energy per unit volume of the film Ω. The anisotropic part of the dipole energy gives rise to the shape anisotropy and demagnetization effects in ferromagnets. This, in turn, causes the *externally* measured susceptibility to be insensitive to the divergence of the *internal* susceptibility at the Curie temperature

T_C of a perpendicularly magnetized film.[24] With no contribution from critical fluctuations at T_C, the susceptibility is dominated by domain formation driven by the isotropic, antiferromagnetic dipole interaction between distant spins.

The density n of the magnetic domains is governed by balancing the dipole energy gained by domain formation against the energy cost of inserting a domain wall. It is given by[2,3,5]

$$n = \frac{c}{l}\exp\left(-\frac{\pi E_{\text{wall}}}{2\Omega t}\right), \tag{1}$$

where t is the film thickness and $c \approx 2$ is a constant whose exact value depends on approximations within the derivation. E_{wall} is the energy per unit area of the domain wall, and l is the width of the domain wall:

$$E_{\text{wall}} = 4\sqrt{\Gamma K_{\text{eff}}}, \tag{2}$$

$$l = \pi\sqrt{\frac{\Gamma}{K_{\text{eff}}}}. \tag{3}$$

In these expressions Γ is the exchange energy per unit length due to the relative rotation of neighboring spins within the domain wall, and K_{eff} is the effective magnetic anisotropy per unit volume. K_{eff} is given by the difference in energy when the magnetization is aligned perpendicular to vs parallel to the surface. $K_{\text{eff}} = K - \Omega$ has contributions from both the crystalline anisotropy per unit volume K (favoring a perpendicular moment in these films), and the anisotropic dipole term (which favors an in-plane moment). All the magnetic quantities are implicit functions of temperature, so that when the temperature is varied, K_{eff} changes and the domain density varies exponentially. If $K_{\text{eff}} \to 0$, a spin reorientation transition occurs.[25,26]

If the domain walls are free to move, they respond to the applied magnetic field in a susceptibility measurement and give an equilibrium susceptibility[3] $\chi^{\text{eq}} \sim 1/n$. However, inhomogeneities in the films can serve to pin the domain walls so that, on average, the walls move toward the equilibrium state with a relaxation time τ. The motion of the walls is a thermally activated process whereby parts of the walls become trapped in ''pinning sites'' with a distribution of activation energies centered at E_a. For a compact distribution, τ is given by an Arrenhius law as[8]

$$\tau(T) = \tau_0 \exp\left(\frac{E_a}{k_B T}\right), \tag{4}$$

where τ_0 is a constant. In measurements of the magnetic susceptibility, a magnetic field is applied at a frequency ω but the walls do not respond instantaneously. Assuming that the magnetization responds linearly to the departure from equilibrium yields[16,17]

$$\chi(T) = \frac{1 - i\omega\tau(T)}{1 + \omega^2\tau^2(T)}\chi^{\text{eq}}(T). \tag{5}$$

The real part of the susceptibility exhibits a broad peak at the temperature T_p, where $\omega\tau(T_p) \sim 1$. Above the peak the walls are freely moving, but below it their motion is thermally activated.

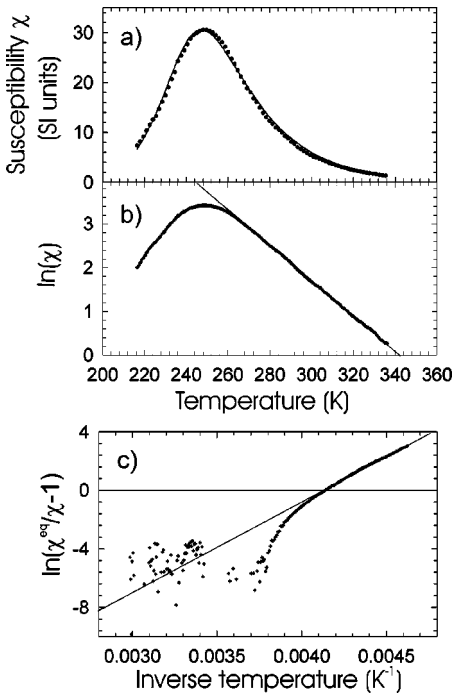

FIG. 1. (a) The susceptibility of a 1.5 ML Fe/2 ML Ni/W(110) film which has been annealed to 375 K. Only every fifth data point is plotted to allow the line derived from the fits in parts (b) and (c) to be seen. (b) At high temperature, the susceptibility has a logarithmic dependence from which the parameter κ in Eq. (6) may be fit. (c) At low temperature an Arrenhius plot gives the activation energy.

Figure 1 shows the real part of the susceptibility (measured in phase with the field applied perpendicular to the surface at 210 Hz) for a 1.5 ML Fe/2 ML Ni/W(110) film which has been annealed to 375 K. In Fig. 1(a) the data is plotted on a linear scale, whereas a semilogarithmic scale is used in Fig. 1(b). The susceptibility due to freely moving domains, above $T \sim 260$ K does indeed show an exponential decrease as predicted by Eq. (1) for decreasing K_{eff}. Since the precise dependence of the argument of the exponential on temperature is controlled by $K_{\text{eff}}(T)$, it is very difficult to calculate from first principles. However, this data is representative of all the measurements in that it is well approximated by the expression

$$\chi^{\text{eq}}(T) = Ae^{-\kappa T} + B. \tag{6}$$

Because $\chi^{\text{eq}} \sim 1/n$, the phenomenological constant κ represents the linear term in the expansion of the temperature dependence of the exponent in Eq. (1):

$$\kappa = \frac{\pi E_{\text{wall}}}{2\Omega t}\left(\frac{1}{2K_{\text{eff}}}\frac{\partial K_{\text{eff}}}{\partial T} + \frac{1}{2\Gamma}\frac{\partial \Gamma}{\partial T} - \frac{1}{\Omega}\frac{\partial \Omega}{\partial T}\right)_{T=T_0}. \tag{7}$$

The curve fitted to the data in Fig. 1(b) uses $\kappa = 0.0421 \pm 0.0006\,K^{-1}$ and B is indistinguishable from zero. These values are the order of magnitude predicted by simple models.[2,16] Figure 1(c) shows the data plotted as

$$\ln\left(\frac{\chi^{\mathrm{eq}}(T)}{\chi(T)}-1\right)=2\ln(\omega\tau_0)+2\frac{E_a}{T} \tag{8}$$

vs $1/T$, so that the activation energy can be extracted from the slope at low temperature. This gives $E_a=3190\pm20$ K for this trace. Using these fitted parameters in Eq. (5) yields the curve plotted with the data in Fig. 1(a).

The activation energy can be interpreted in terms of the magnetic properties using a theory due to Bruno *et al.*[8] They model the pinning of domain walls as a one-dimensional sinusoidal effective potential with a peak-to-peak amplitude given by E_a. The mean characteristic length associated with the pinning sites is ξ. In ultrathin films, the pinning may be caused by variations ΔE_{wall} in the domain wall energy due to thickness variations as small as 1 ML, as this can represent a large proportion of the total thickness. Close to the reorientation transition in perpendiculary magnetized films, where $K_{\mathrm{eff}}\rightarrow0$, the domain wall width in Eq. (3) gets very large. If $l\sim\xi$, the domain wall averages over the pinning sites and reduces ΔE_{wall} by a factor of ξ/l. Then[8]

$$E_a=\frac{t\xi}{E_{\mathrm{wall}}}\left(\frac{\xi}{l}\Delta E_{\mathrm{wall}}\right)^2. \tag{9}$$

This model has been used successfully to describe pinning as a function of film thickness with thickness steps of 1 ML.[8,16]

III. EXPERIMENT AND SAMPLE CHARACTERIZATION

The films were grown using molecular beam epitaxy in a UHV system with a base pressure of 2×10^{-10} Torr. A W(110) single crystal with a miscut less than 0.4° was cleaned by cycles of heating in oxygen and flashing to 2600 K. The growth of the films is described in detail elsewhere.[27] The first layer of Ni was evaporated with the substrate at 550 K and was then annealed to 700 K. A second Ni layer was grown at 360 K, followed by iron deposition at 350 K. The films show a perpendicular moment up to the Curie temperature when the iron thickness $\leqslant2$ ML.[28] Some information on the fine scale structure of the films is available. The 2 ML Ni seed layer wets the tungsten substrate very well,[29] and the Fe grows nearly layer-by-layer.[27] The LEED patterns are sharp up to 3 ML Fe growth, after which a gradual evolution to bcc iron occurs and is completed by 12 ML. Some mixing of the last Ni layer and the first Fe layer, as grown, was found using angle-resolved Auger electron spectroscopy.[30] The amount of mixing is approximately 15%.

The ac magnetic susceptibility of the film was measured *in situ* using the surface magneto-optical Kerr effect (SMOKE) in the perpendicular geometry. The apparatus has been described in detail elsewhere.[31] The ac magnetic field was applied perpendicular to the surface using a frequency of 210 Hz and a peak amplitude of 12.5 Oe. Tests using a smaller field amplitude confirmed that the shape of the real part of the susceptibility curve was not distorted by nonlinear field effects. However, unexplained quantitative discrepancies between the theoretical and observed imaginary part of the susceptibility (not discussed here) could indicate a departure from linear response. The susceptibility was measured as a function of temperature from 200 to 350 K, and Auger electron spectra of the tungsten peaks (150–190 eV) and the iron and nickel peaks (35–75 eV) were recorded to provide information about the morphology, thickness, and distribution of the iron and nickel. The film was then annealed to successively higher temperatures for one minute and the measurements were repeated.

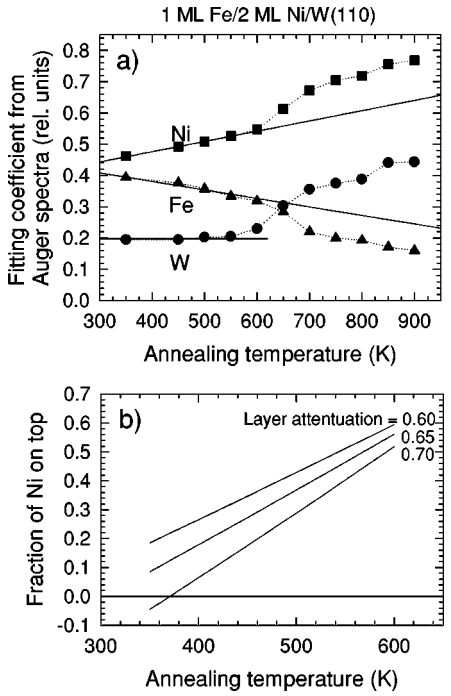

FIG. 2. (a) The coefficients for fitting Auger electron spectra to a linear combination of basis spectra for a bare substrate and thick film, are plotted as a function of the temperature to which the film has been annealed. For annealing below 600 K, the linear change in the Ni and Fe coefficients, while the coefficient for the W substrate remains constant, indicates that the Fe/Ni interface is being mixed. (b) The amount of Ni in the top layer implied by the mixing seen in part (a), according to a model described in the text. Curves for different assumed inelastic mean free paths of the Auger electrons are shown.

In order to infer the structural changes upon annealing, each Auger electron spectrum of the iron and nickel peaks was fit to a linear combination of the spectra for a bare 2 ML Ni/W(110) film and a 3 ML Fe/2ML Ni/W(110) film. The coefficients of the fits for a 1 ML Fe/2 ML Ni/W(110) film are plotted as a function of the annealing temperature in Fig. 2(a). The attenuation of the tungsten spectra were found by comparison to a spectrum taken from clean W(110). At and below an annealing temperature of 550 °C, the constant tungsten signal indicates that the thickness of the films is not changing. Above 550 °C, the rapid increase in both the tungsten and nickel signals, accompanied by a decrease in the iron signal, indicates that the iron layer and the top nickel layer are forming thicker islands on top of 1 ML Ni/W(110), which is stable up to much higher temperatures. This interpretation is confirmed by the appearance of the distinctive reconstructed LEED pattern of 1 ML Ni/W(110) in this range of annealing temperatures.[32] Results for a 2 ML film were similar.

Below 550 K, the more gradual change in the Ni and Fe Auger electron signals suggests that mixing is occurring, with Ni coming to the top layer, and Fe moving to the second layer. The roughly linear trend in the data begins at the

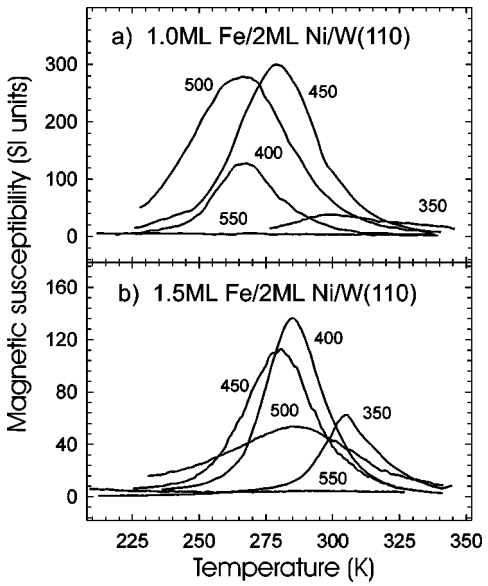

FIG. 3. The measured susceptibility of two films which have been stepwise annealed to the temperatures (K) indicated beside each trace. (a) is for a 1 ML Fe film and (b) is for a 1.5 ML Fe film.

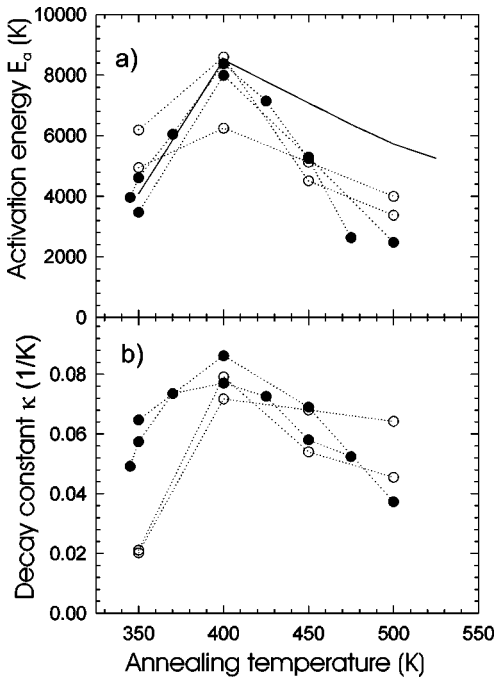

FIG. 4. (a) Activation energies E_a and (b) decay constants κ of films as a function of the annealing temperature. The open symbols are for 1 ML Fe films, and the solid symbols are for 1.5 ML Fe films. The solid line in (a) is the model described in the text.

growth temperature, confirming that some mixing occurs in the films as grown. An estimate of the degree of mixing can be made using the data in Fig. 2(a) and the exponential attenuation of Auger electrons with thickness. Using the lines fitted to the linear portions of the curves in Fig. 2(a), the Auger signal $I(T_a)$ after annealing to temperature T_a was expressed as the linear combination

$$I(T_a)=\alpha I_{3\mathrm{Fe}/2\mathrm{Ni}}+\beta I_{2\mathrm{Ni}}. \tag{10}$$

To infer mixing, the signal was also modeled as a linear combination of basis spectra from 1 ML Fe/2 ML Ni and 1 ML Ni/1 ML Fe/1ML Ni films

$$I(T_a)=\gamma I_{\mathrm{Fe}/2\mathrm{Ni}}+\delta I_{\mathrm{Ni}/\mathrm{Fe}/\mathrm{Ni}}. \tag{11}$$

The coefficients α and β are related to γ and δ by summing the expected Auger electron signal from each layer, with appropriate attenuation by $\exp(-b/\lambda)$ per layer on top of the emitting atom. In this expression, b is the thickness of one layer and λ is the inelastic mean free path. The degree of mixing is then given by $\delta/(\gamma+\delta)$. Choosing a small range of inelastic mean free path consistent with the ''universal'' curve,[33] gives fractional mixing of the iron and nickel which lies within the physically possible range of 0 to 50%. These are shown in Fig. 2(b). In particular, choosing a value of $\exp(-b/\lambda)=0.65$ gives mixing near 15% for the as-grown films (in agreement with experiment) and mixing of near 50% at an annealing temperature of 550 K where large scale motion of the upper layers occurs. This internal consistency suggests that Fig. 2(b) gives a reasonable estimate of the mixing of the top two monolayers as a function of the annealing temperature.

IV. RELATION OF THE DOMAIN PROPERTIES AND FILM MICROSTRUCTURE

The magnetic susceptibilities for two representative films are shown as a function of annealing temperature in Fig. 3. They illustrate a behavior found in all the measurements—the first annealing step above the growth temperature results in a sudden downward shift ($\sim$40 K) in the temperature at which the susceptibility peaks, accompanied by a substantial increase in the peak value of χ and a decrease in the peak width. Subsequent annealing steps produce a more continuous evolution of the susceptibility, with the peak temperature varying less. Finally, the susceptibility disappears upon annealing to 550 K. These different behaviors suggest that there are three different microstructural changes involved. While the first annealing step produces little additional interface mixing, it is likely to allow lateral motion of surface atoms and to reduce surface roughness. This could cause the initial shift in χ. Subsequent annealing causes incremental mixing at the interface, giving a more continuous evolution of χ. Finally, Fig. 2(a) indicates that at and above an annealing temperature of 550 K, where the susceptibility disappears, the film structure breaks down. The lack of magnetic response may be due to a superparamagnetic response of the thicker islands above the blocking temperature. It may also be because the remaining 1 ML Ni/W(110) is magnetized in-plane or has a Curie temperature below 200 K.

A quantitative analysis of the susceptibility curves supports these ideas. Each curve was fit to Eqs. (5) and (6), using the method illustrated in Fig. 1. The resulting values of E_a and κ are plotted in Fig. 4 as a function of annealing temperature. All the films exhibit an initial increase in both E_a and κ, followed by a continuous decrease upon annealing above 400 K. This clear and consistent reversal strongly suggests two different mechanisms related to the film microstructure. In the case of the activation energy, it is reasonable that a reduction in surface roughness during the first annealing step would increase ξ, the mean separation of domain pinning sites, and lead to an increase in E_a in Eq. (9). When

mixing occurs at higher annealing temperatures, the iron/vacuum interface which supports a perpendicular surface anisotropy will be partially replaced by a nickel/vacuum interface which favors an in-plane surface anisotropy.[36] According to Eqs. (9) and (2), a reduction in the surface anisotropy will reduce the activation energy.

It is more difficult to comment on the detailed behavior of κ, since analysis using Eq. (7) requires knowledge of the temperature dependence of magnetic quantities for the structure at each annealing temperature. Qualitative arguments can be made by noting that the temperature dependence within the brackets should be relatively insensitive to annealing, since all the temperature derivatives are self-normalized and all the measurements of κ are made in the same temperature range. (While the anisotropy term has a significant temperature derivative, it is the normalized change in this derivative between annealing steps which is relevant.) Therefore, changes in κ upon annealing should be governed mostly by the prefactor. As the interface mixing occurs, the surface anisotropy is reduced and so is the prefactor in Eq. (7), in agreement with the data. However, the initial increase in κ observed for lower annealing temperatures is unexpected. Since κ is related to the rate of change of the density of *freely moving* domain walls, it should not depend upon changes in the surface roughness.

In order to further test these ideas, model calculations of $K(T_a)$, $\Gamma(T_a)$, and $\Omega(T_a)$ have been performed. The model consists of a 3 ML fcc film where the first ML of Ni remains at the interface of W(110) because of its greater thermal stability. The second monolayer of Ni and top monolayer of Fe mix by random atomic exchange. Thus the annealed films have a top layer with a fraction δ of Ni atoms and $(1-\delta)$ of Fe atoms, and a second layer with reversed concentrations. No correlated movements of blocks of atoms occur. Since all the magnetic atoms in the ultrathin films studied here are at either a surface or interface, each has a first order contribution to the magnetic anisotropy due to nearest neighbor interactions in the Néel model.[34] The volume anisotropy due to longer range interactions, and any contributions due to strain are neglected. In this approximation, $K=K_s/t$, where K_s is the surface anisotropy per unit area. The explicit thickness dependence in this model can be used to evaluate ΔE_{wall} by differentials using Eq. (2). Then Eq. (9) yields

$$E_a=\frac{t\xi^3}{\pi^2\sqrt{\Gamma K_{\text{eff}}}}\left(\frac{K_s}{t}\right)^2\left(\frac{\Delta t}{t}\right)^2. \tag{12}$$

The surface anisotropy is interpolated from experimental data using the formalism of Néel's pair model.[35] The surface anisotropy contributed by the ith magnetic atom is given by

$$K_i=\sum_j^{\text{NN}} \eta L_{i,j}(\hat{\boldsymbol{r}}_{i,j}\cdot\hat{\boldsymbol{M}})^2, \tag{13}$$

where $L_{i,j}$ is the coupling constant with nearest-neighbor atoms j, $\hat{\boldsymbol{r}}_{i,j}$ is a unit vector joining these atoms, and $\hat{\boldsymbol{M}}$ is a unit vector in the direction of the magnetization. η is equal to 1/2 when both atoms are magnetic or is equal to 1 when only one atom is magnetic; this eliminates double counting of the pairwise interactions. For the case of a perfectly ordered fcc (111) interface or surface between magnetic (m) and nonmagnetic (n) atoms, the Néel model gives

$$K_s=\frac{3}{4}(L_{m,m}-2L_{m,n})\sin^2\theta, \tag{14}$$

where θ is the angle between the magnetization and the surface normal. When the perfectly ordered interface is between two magnetic species

$$K_s=\frac{3}{4}(L_{m1,m1}-2L_{m1,m2}+L_{m2,m2})\sin^2\theta. \tag{15}$$

The values of the pair coupling $L_{i,j}$ were derived from experimental values of the surface anisotropy at room temperature. Using K_s from vacuum/Ni(111),[36] vacuum/Ni/W(110),[36] vacuum/Fe/Ni/W(110),[37] vacuum /Fe/Cu(111),[38] and Fe/Cu(111) (Ref 39) interfaces in Eqs. (14) and (15) allows the extraction of $L_{\text{Ni,Ni}}=-0.25$ meV/atom, $L_{\text{Fe,Fe}}=0.53$ meV/atom, $L_{\text{Ni,W}}=-0.19$ meV/atom, and $L_{\text{Fe,Ni}}=0.18$ meV/atom near room temperature. [The Fe/Cu data is used to obtain approximate values for fcc(111) Fe.] The anisotropy for the mixed film can now be found by summing Eq. (13), and the difference in the anisotropy for magnetization perpendicular to and in the surface plane is plotted in Fig. 5(a). The three

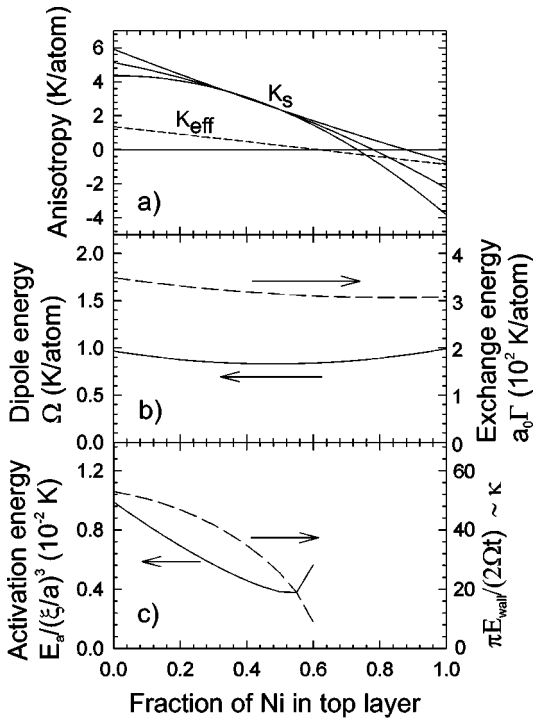

FIG. 5. Calculated magnetic energies of a 1 ML Fe/ 2 ML Ni/ W(110) film as function of the mixing of the top two layers. (a) The surface anisotropy K_s is interpolated from experimental data using Néel's model. The three solid curves give a range spanned by the experimental uncertainties. The effective anisotropy K_{eff} is plotted as a dashed line. (b) The anisotropic dipole energy (left scale) and exchange energy in the domain walls (right scale). (c) The activation energy of pinning sites according to Eq. (12) is shown by the solid line. The dependence on the pinning correlation length ξ has been removed. The dashed line gives the prefactor to Eq. (7), which is related to variations in κ.

curves indicate a range allowed by the quoted errors in the experimental results. The curve moves from positive anisotropy when the top layer is primarily Fe to negative anisotropy when the top layer is primarily Ni and the magnetization would lie in-plane. While the systems are not strictly comparable, this is similar to measurements of K_s in FeNi alloy films on Cu(111).[40]

The exchange constant Γ is also related to a nearest neighbor pairwise interaction, the Heisenberg exchange integral $J_{i,j}$. The Ni and Fe spins are treated as classical vectors $\boldsymbol{S}_i$ aligned at zero temperature. The quadratic dispersion constant of spin waves at small wave vector[41] ($\sim 2JS$) and the magnetic moments ($\sim g_s \mu_B S$) were used to calculate $J_{\mathrm{Ni,Ni}}|\boldsymbol{S}_{\mathrm{Ni}}|^2 = 51\,\mathrm{K}$ and $J_{\mathrm{Fe,Fe}}|\boldsymbol{S}_{\mathrm{Fe}}|^2 = 218\,\mathrm{K}$. An approximate value for $J_{\mathrm{Ni,Fe}}\boldsymbol{S}_{\mathrm{Ni}} \cdot \boldsymbol{S}_{\mathrm{Fe}}$ is found by scaling $J_{\mathrm{Ni,Ni}}|\boldsymbol{S}_{\mathrm{Ni}}|^2$ by the ratio of T_c for ultrathin equal concentration FeNi alloy films and Ni films.[42] For layered and mixed films, an average exchange can be defined as

$$\frac{1}{2} J_{\mathrm{eff}} |\boldsymbol{S}_{\mathrm{eff}}|^2 = \frac{1}{2N_b} \sum_i^N \sum_j^{\mathrm{NN}} J_{i,j} \boldsymbol{S}_i \cdot \boldsymbol{S}_j , \tag{16}$$

where j runs over the nearest neighbors of the atom at site i, and N_b is the number of nearest-neighbor bonds in the sum. For an fcc structure with conventional cubic cell length of a_0, the exchange energy per unit length of domain wall is[43]

$$\Gamma = \frac{4}{a_0} J_{\mathrm{eff}} |\boldsymbol{S}_{\mathrm{eff}}|^2 . \tag{17}$$

This result is plotted in Fig. 5(b) as the dashed line. It shows little variation with mixing, in agreement with experimental studies of ultrathin NiFe alloy films,[42] which show no fcc to bcc structural change with alloy concentration, and only modest changes in T_c.

Finally, the effect of mixing on the shape anisotropy was calculated, using the anisotropic term in the dipole energy. In order to average over all atomic configurations, effective atoms with a moment $\mu = \delta \mu_{\mathrm{Ni}} + (1-\delta)\mu_{\mathrm{Fe}}$ were used, for example, in the top layer. The result is also shown in Fig. 5(b) as the solid line. Because of the long range nature of the dipole interaction, this term depends very little on mixing. Since the susceptibilities were measured at $\sim 270 \pm 30\,\mathrm{K}$ and the measurements of K_s were made near room temperature as well, the dipole term must be corrected to this temperature before K_{eff} can be formed. Using[28] $T_c \sim 325 \pm 20\,\mathrm{K}$, and the Ising exponent $\beta = 1/8$ gives $\Omega = 0.64\Omega(T=0)$, and results in K_{eff} as shown as the dashed line in Fig. 5(a). Values of K_s near the upper boundary allowed by the experimental error in Fig. 5(a) have been chosen for this calculation. In this way $K_{\mathrm{eff}} \rightarrow 0$ for a Ni rich top layer and no spin reorientation is predicted upon annealing, in agreement with the traces in Fig. 3.

Placing all these results in Eq. (12) gives the activation energy as a function of the mixing of the top two layers for $\Delta t = 1$ ML. This is shown in Fig. 5(c). [A factor of $(\xi/a)^3$ is removed, where a is the nearest-neighbor distance.] The simple model calculation indeed shows that E_a falls quickly and continuously upon mixing of the Fe and Ni layers. Only for Ni rich surfaces beyond equal mixing does the curve begin to increase due to the predicted reorientation. Also shown in Fig. 5(c) is the prefactor of Eq. (7), which should approximate the relative changes in κ. Since this depends on a lower power of K_s than the activation energy, it falls more slowly with mixing, in qualitative agreement with the experimental results.

These results can be compared to the annealing experiments by using the approximate correspondence between mixing and annealing temperature in Fig. 2(b). Choosing ξ/a near 110 for the annealed films, and 75 for the as-grown films, gives the model curve for the activation energy plotted in Fig. 4(a). The good qualitative agreement confirms that the interface mixing is driving the changes in domain properties. A closer quantitative agreement can be easily achieved by increasing K_s or decreasing $\Omega(T)$, but given the approximations involved in the calculation detailed fitting to the data is not justified. These values give $(\xi/a)(\Delta E_{\mathrm{wall}}/E_{\mathrm{wall}}) \sim 1/2$ and Bruno's model of the pinning potential, which is based on an expansion using this parameter, is within a valid range. Then $\xi \sim 275\,\text{Å}$, within the range of pinning correlation lengths seen in other studies.[8,12,14] If ξ is identified with an island size or terrace length, then the films are very smooth and the changes in anisotropy due to surface roughness are negligible.[18,19] The good qualitative agreement between the calculation and the measurements support the model of Bruno *et al.*, and indicates a direct link between surface smoothing and interface mixing and the changes in the domain wall properties.

In a further test of these ideas, films were intentionally grown with a morphology which differed from those analyzed above. For these films, the first monolayer of Ni was *not* annealed before subsequent Ni and Fe layers were grown. This is known to produce a Ni substrate with more incomplete layer filling and a much greater island nucleation density,[29] and should lead to more interface mixing and a shorter separation of pinning sites in the film as grown. The susceptibility measured for this film is shown in Fig. 6(b), labeled ''A.'' The peak is approximately 80 K lower in temperature than the films in Fig. 3 (it was not possible to find E_a because of the limitations of the sample cooling arrangement), and illustrates again the sensitivity of the domain formation to film morphology.

As a result of this sensitivity, the dependence of the peak temperature upon the film thickness first presented in Ref. 28 has been remeasured. These results are given in Fig. 6(a), where the solid symbols represent measurements from the earlier investigation and the open and cross symbols are the present measurements. The cross symbols represent films where annealing of the first Ni layer was intentionally omitted. At low temperature the films are perpendicularly magnetized, with the plotted peaks showing roughly where the perpendicular domains become freely moving. At Fe thicknesses greater than 2 ML, the domain phase leads to a spin reorientation transition, with the region of in-plane magnetism sketched using a dashed line.[28] The lines through the data are guides to the eye. An unexplained dip in the peak temperature near thicknesses of 1 ML seen in the earlier data is not reproduced. Comparison of the susceptibility measured earlier for a thickness of 1.25 Fe ML (labeled ''B'' in Fig. 6) to that measured without annealing the first Ni layer (labeled ''A'') suggests that the dip was the result of an unintentional

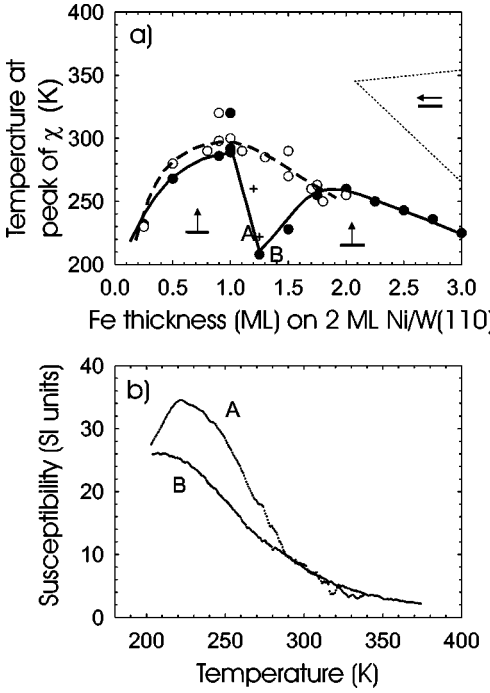

FIG. 6. (a) The temperature at the peak of the susceptibility is plotted as a function of the Fe thickness. Solid symbols are data from Ref. 24, and open and cross symbols are data from the present study. The cross symbols are from films where the first Ni layer was not annealed. (b) The susceptibility for the points labeled A and B.

variation in the sample growth procedure for a few points in this very sensitive thickness regime.

A more subtle question is the cause of the topological similarity of the plot in Fig. 6(a) (once points B are omitted) to the phase diagram for the spin reorientation transition.[36,44] The present studies, and others,[8,16] suggest an indirect linkage through the magnetic anisotropy. A decrease in the anisotropy decreases the activation energy, and thus lowers the temperature at which the susceptibility has its maximum. Similarly, a decrease in the anisotropy leads to a lower temperature for the reorientation transition. That this indirect tracking of the reorientation by domain properties depends sensitively on the way in which sample morphology affects the domain properties is not surprising.

V. CONCLUSIONS

Analysis of Fe films grown on 2 ML Ni/W(110) has demonstrated again that interfacial smoothness has a profound effect on magnetic properties of ultrathin films—in this instance upon the formation and motion of domain walls in perpendicularly magnetized films. The magnetic susceptibility of 1–1.5 ML Fe films was found to be dominated by domain wall motion, and a simple analysis yields the activation energy of sites which pin domain walls, and the temperature dependence of the equilibrium domain concentration. The susceptibility and activation energy are strongly dependent upon the temperature to which the films are annealed, and thus upon the smoothing and interface mixing that annealing produces.

Qualitative and quantitative analysis of the data, and calculations based upon the model of Bruno *et al.*,[8] provide a consistent picture of the link between the domain wall properties and the film structure. Pinning is caused by changes in the domain wall energy at atomic steps. Annealing of the as-grown films increases the mean separation of pinning sites and leads to an initial increase in the activation energy. Further annealing causes mixing of the Fe/Ni interface, which reduces the activation energy by reducing the surface anisotropy. The reduction of the surface anisotropy also leads to an increase in the equilibrium domain density. After annealing to a sufficiently high temperature the film breaks up to form thicker islands which do not give a magnetic response in the temperature range accessible in these experiments.

ACKNOWLEDGMENTS

We are pleased to thank M. Kiela for technical assistance with the experiments and C. S. Arnold for a critical review of the manuscript. This research was supported by the Natural Sciences and Engineering Research Council of Canada.

[1] B. Kaplan and G.A. Gehring, J. Magn. Magn. Mater. **128**, 111 (1993).
[2] A.B. Kashuba and V.L. Pokrovsky, Phys. Rev. B **48**, 10 335 (1993).
[3] Ar. Abanov, V. Kalatsky, V.L. Pokrovsky, and W.M. Saslow, Phys. Rev. B **51**, 1023 (1995).
[4] P. Politi, Comments Condens. Matter Phys. **18**, 191 (1998).
[5] R. Skomski, H.-P. Oepen, and J. Kirschner, Phys. Rev. B **58**, 3223 (1998). This paper also calculates that in the monolayer limit this argument fails, and the film will be a single domain.
[6] V. Gehanno, Y. Samson, A. Marty, B. Giles, and A. Chamberod, J. Magn. Magn. Mater. **172**, 26 (1997).
[7] A. Berger and R.P. Erickson, J. Magn. Magn. Mater. **165**, 70 (1997).
[8] P. Bruno, G. Bayreuther, P. Beauvillain, C. Chappert, G. Luget, D. Renard, and J. Seiden, J. Appl. Phys. **68**, 5759 (1990).
[9] R. Allenspach, M. Stampanoni, and A. Bischof, Phys. Rev. Lett. **65**, 3344 (1990).
[10] R. Allenspach and A. Bischof, Phys. Rev. Lett. **69**, 3385 (1992).
[11] M. Speckmann, H.P. Oepen, and H. Ibach, Phys. Rev. Lett. **75**, 2035 (1995).
[12] A. Kirilyuk, J. Ferré, V. Grolier, J.P. Jamet, and D. Renard, J. Magn. Magn. Mater. **171**, 45 (1997).
[13] A. Berger and H. Hopster, Phys. Rev. Lett. **76**, 519 (1996).
[14] P. Rosenbusch, J. Lee, G. Lauhoff, and J.A.C. Bland, J. Magn. Magn. Mater. **172**, 19 (1997).
[15] P. Poulopoulos, M. Farle, U. Bovensiepen, and K. Baberschke, Phys. Rev. B **55**, R11 961 (1997).
[16] D. Venus, C.S. Arnold, and M. Dunlavy, Phys. Rev. B **60**, 9607 (1999).
[17] C.S. Arnold and D. Venus, IEEE Trans. Magn. **34**, 1029 (1998).
[18] P. Bruno, J. Appl. Phys. **64**, 3153 (1988).
[19] P. Bruno, J. Phys. F: Met. Phys. **18**, 1291 (1988).
[20] R. Arias and D.L. Mills, Phys. Rev. B **59**, 11 871 (1999).

[21] I. Booth, A.B. MacIsaac, J.P. Whitehead, and K. De'Bell, Phys. Rev. Lett. **75**, 950 (1995).
[22] W. Wulfhekel, S. Knappmann, B. Gehring, and H.P Oepen, Phys. Rev. B **50**, 16 074 (1994).
[23] G. Garreau, M. Farle, E. Beaurepaire, and K. Baberschke, Phys. Rev. B **55**, 330 (1997).
[24] H.B. Callen, *Thermodynamics* (Wiley, New York, 1960), Sec. 4.4.
[25] H. Fritzsche, J. Kohlhepp, H.J. Elmers, and U. Gradmann, Phys. Rev. B **49**, 15 665 (1994).
[26] Y. Millev and J. Kirschner, Phys. Rev. B **54**, 4137 (1996).
[27] H.L. Johnston, C.S. Arnold, and D. Venus, Phys. Rev. B **55**, 13 221 (1997).
[28] C.S. Arnold, H.L. Johnston, and D. Venus, Phys. Rev. B **56**, 8169 (1997).
[29] D. Sander, A. Enders, C. Schmidthals, J. Kirschner, H.L. Johnston, C.S. Arnold, and D. Venus, J. Appl. Phys. **81**, 4702 (1997).
[30] H.L. Johnston, Ph.D. thesis, McMaster University, 1997.
[31] C.S. Arnold, M. Dunlavy, and D. Venus, Rev. Sci. Instrum. **68**, 4212 (1997).
[32] K.-P. Kämper, W. Schmitt, G. Güntherodt, and H. Kuhlenbeck, Phys. Rev. B **38**, 9451 (1988).
[33] A. Zangwill, *Physics at Surfaces* (Cambridge University Press, Cambridge, 1988), Chap. 2.
[34] L. Néel, J. Phys. Radium **15**, 376 (1954).
[35] H.J. Draaisma, F.J.A. den Broeder, and W.J.M. de Jonge, J. Appl. Phys. **63**, 3479 (1988).
[36] M. Farle, Rep. Prog. Phys. **61**, 755 (1998).
[37] H. Höche and H.-J. Elmers, J. Magn. Magn. Mater. **191**, 313 (1999). We have reanalyzed this data to include only Fe thicknesses less than 10 ML, because of the known fcc to bcc transformation. Then one obtains $K_s = 1.3 \pm 0.2\ \mathrm{mJ/m^2}$ and a room temperature reorientation transition for a pseudomorphic thickness of 2.1 Fe ML, in agreement with Ref. 28.
[38] P. Ohresser, J. Shen, J. Barthel, M. Zheng, Ch.V. Mohan, M. Klaua, and J. Kirschner, Phys. Rev. B **59**, 3696 (1999).
[39] L. Smardz, B. Szymański, J. Barnaś, and J. Baszyński, J. Magn. Magn. Mater. **104-107**, 1885 (1992).
[40] U. Gradmann and H.-J. Elmers, J. Magn. Magn. Mater. **206**, L107 (1999).
[41] C. Kittel, *Introduction to Solid State Physics* (Wiley, New York, 1986), Chap. 15.
[42] F.O. Schumann, S.Z. Wu, G.J. Mankey, and R.F. Willis, Phys. Rev. B **56**, 2668 (1997).
[43] S. Chickazumi, *Physics of Magnetism* (Wiley, New York, 1964), Chap. 9.
[44] P. Politi, A. Rettori, M.G. Pini, and D. Pescia, J. Magn. Magn. Mater. **140-144**, 647 (1995).